ORIGINAL PAPER

Astaxanthin reduces hepatic endoplasmic reticulum stress and nuclear factor-κB-mediated inflammation in high fructose and high fat diet-fed mice

Saravanan Bhuvaneswari · Baskaran Yogalakshmi · S. Sreeja · Carani Venkatraman Anuradha

Abstract We recently showed that astaxanthin (ASX), a xanthophyll carotenoid, activates phosphatidylinositol 3-kinase pathway of insulin signaling and improves glucose metabolism in liver of high fructose–fat diet (HFFD)-fed mice. The aim of this study is to investigate whether ASX influences phosphorylation of c-Jun-N-terminal kinase 1 (JNK1), reactive oxygen species (ROS) production, endoplasmic reticulum (ER) stress, and inflammation in liver of HFFD-fed mice. Adult male *Mus musculus* mice were fed either with control diet or HFFD for 15 days. After this period, mice in each group were divided into two and administered ASX (2 mg/kg/day, p.o) in 0.3 ml olive oil or 0.3 ml olive oil alone for the next 45 days. At the end of 60 days, liver tissue was excised and examined for lipid accumulation (Oil red O staining), intracellular ROS production, ER stress, and inflammatory markers. Elevated ROS production, lipid accumulation, and increased hepatic expression of ER stress markers such as Ig-binding protein, PKR-like ER kinase, phosphorylated eukaryotic initiation factor 2α, X-box binding protein 1, activating transcription factor 6, and the apoptotic marker caspase 12 were observed in the liver of the HFFD group. ASX significantly reversed these changes. This reduction was accompanied by reduced activation of JNK1 and I kappa B kinase β phosphorylation and nuclear factor-kappa B p65 nuclear translocation in ASX-treated HFFD mice. These findings suggest that alleviation of inflammation and ER stress by ASX could be a mechanism responsible for its beneficial effect in this model. ASX could be a promising treatment strategy for insulin resistant patients.

Keywords Astaxanthin · High fructose–fat diet · ER stress · Inflammation · Reactive oxygen species

S. Bhuvaneswari · B. Yogalakshmi · S. Sreeja ·
C. V. Anuradha (✉)
Department of Biochemistry and Biotechnology, Annamalai University, Annamalai Nagar 608 002, Tamil Nadu, India
e-mail: cvaradha@hotmail.com

Introduction

Insulin resistance, defined as the reduced response of tissues to circulating insulin, is the core pathogenic factor in type 2 diabetes (T2D) and obesity (Lebovitz 2001). The metabolic actions of insulin are mediated by a pathway involving insulin receptor substrates (IRS), phosphatidylinositol-3-kinase (PI3K) and Akt (IRS-PI3K-AKT signaling pathway). Binding of insulin to its receptor (IR β) activates tyrosine phosphorylation of IR β and its substrates (IRS 1–4). Insulin resistance occurs when there is a downregulation of the IRS1-PI3K-AKT pathway. Studies show that serine phosphorylation of insulin receptor and its substrates (IRS)-1 and 2 leads to a block in tyrosine phosphorylation resulting in abrogation of insulin signaling (Schaffer 2003). Various serine kinases, such as c-Jun NH$_2$-terminal kinase (JNK), inhibitor kappa kinase beta (IKKβ), and others have been implicated in the serine phosphorylation of IRS-1(Draznin 2006). These kinases are activated following signaling by inflammatory cytokines, reactive oxygen species (ROS), and lipids and lipid metabolites (Tanti and Jager 2009; Perseghin et al. 2003).

Endoplasmic reticulum (ER) plays an important role in the assembly and folding of nascent polypeptides by providing an optimized environment for the maturation of cell proteins. During pathophysiological states including obesity, hyperlipidemia, nutrient deprivation, hypoxia, infection, and inflammation, proteins formed in the ER may fail to accomplish correct conformation. The accumulation of misfolded proteins in the ER triggers an adaptive response known as the unfolded protein response (UPR) (Shoelson et al. 2003; Gregor and Hotamisligil 2007). UPR is initiated when a resident chaperone, glucose-regulated protein 78 (GRP78), also known as Bip dissociates from the luminal side of ER in order to assist with the folding of proteins in the ER lumen. Dissociation of Bip causes release and activation of three

distinct mediators, inositol requiring enzyme 1 (IRE1), double-stranded RNA-activated protein kinase-like endoplasmic reticulum kinase (PERK), and activating transcription factor 6 (ATF6). IRE1, a transmembrane receptor protein with endonuclease and kinase functions, autophosphorylates, and initiates the splicing of 26-base intron from the X-box binding protein 1 (XBP1) mRNA. The spliced XBP1 then elicits transcriptional activation of several molecular chaperons. PERK dimerizes, gets phosphorylated, and activated causing phosphorylation of eukaryotic initiation factor (eIF2) α. eIF2α attenuates the rate of translation initiation and also activates UPR target genes through a transcription factor-activating transcription factor (ATF) 4. ATF6, another transcription factor, translocates to the cis-Golgi compartment, where it is cleaved by site-1 and site-2 proteases. Activated cytosolic domain of ATF6 enters the nucleus and activates the genes that augment translation attenuation and degradation of misfolded proteins. All these events result in (1) enhancement of ER protein-folding capacity due to increased expression of chaperones and foldases, (2) inhibition of protein translation for a while, and (3) ER-associated protein degradation of misfolded proteins (Hotamisligil 2010). Prolonged ER stress results in cell death by the apoptotic pathway mediated by caspase-12, an ER localized cysteine protease. Accumulation of Ca^{2+} in response to ER stress activates a calpain that converts procaspase-12 to caspase-12, the active form which initiates a cascade of events culminating in apoptosis and cell death.

Recent studies show that disruption of ER homeostasis leads to chronic UPR response and induces metainflammation and insulin resistance in liver (Yalcin and Hotamisligil 2013). Activated IRE1 recruits the tumor necrosis factor receptor-associated factor 2 (TRAF2) as well as the apoptotic signal regulating kinase 1 (ASK1) to form IRE-1-TRAF2-ASK1 complex, which activates both JNK and nuclear factor kappa B (NF-κB). In addition, ER stress can directly promote NF-κB activation through a PERK–eIF2α-mediated attenuation of translation (Deng et al. 2004). JNK and IKKβ-regulated pathways are two important signaling cascades that lead to insulin resistance. Accumulating evidence also suggests that ER stress and ROS production are closely related events and might be associated with NF-κB activation (Deng et al. 2004). Indeed, UPR has been demonstrated in obese, insulin-resistant humans and rodents (Ozcan et al. 2004; Boden et al. 2008). Nutrient imbalance and excessive lipid storage are shown to be responsible for ER stress during insulin resistance (Ozcan et al. 2004).

Intervention with butylated hydroxylanisole, an antioxidant, improved protein folding and cell survival by reduction in ROS production and ER stress in wild type C57BL/6 mice (Malhotra et al. 2008). This observation provides an important strategy to treat and/or prevent diseases of

protein misfolding using antioxidants. Astaxanthin (ASX) is a powerful antioxidant carotenoid produced by *Haemococcus pluvialis*, a microalgae and is found in fungi, sea foods, flamingos, and quails. ASX is a xenohormetic bioactive compound, the production of which can increase under stress conditions (Vidhyavathi et al. 2008). Xenohormetic plant compounds are suggested to yield benefits to the animals directly or by activating the animal's own stress defense pathways (Hooper et al. 2010). ASX has been reported to show antiinflammatory, antitumor, immunomodulatory, anticancer, and antidiabetic activities (Guerin et al. 2003). ASX is marketed as a dietary supplement and is widely used as a nutraceutical by athletes and sportsmen and as a coloring agent in food industry. Previous studies have revealed its anti-obesity effects in mice fed with high fat diet (Ikeuchi et al. 2007) and antidiabetic effects in db/db mice (Uchiyama et al. 2002). We have shown earlier that ASX limits weight gain, lowers oxidative stress, improves insulin sensitivity, activates the IRS-PI3K-Akt pathway of insulin signaling in liver, and skeletal muscle and curtails lipotoxicity and fatty liver disease in HFFD-fed mice (Bhuvaneswari et al. 2010; Arunkumar et al. 2012). However, whether ASX alleviates NF-κB related inflammation and ER stress has not been verified. This study was, therefore, intended to investigate the effects of ASX on ER stress and inflammation in the liver of HFFD-fed mice.

Materials and methods

Synthetic ASX was purchased from Sigma-Aldrich Pvt. Ltd., MO, USA. Solvents and chemicals of analytical grade were purchased from HiMedia laboratories Pvt. Ltd., Mumbai, India. Anti-PERK and antiphospho-eIF2α antibodies were kindly provided as gift by Prof. Louise Larose, Polypeptide Lab, Rue University, Korea.

Animals and treatment

Adult male *Mus musculus* albino mice of Swiss strain weighing 25–30 g were used for the study. The animals were housed individually under hygienic conditions (22–24 °C) under 12 h light/12 h dark cycle in polypropylene cages. The animals were acquired from and maintained in the Central Animal House, Department of Experimental Medicine, Rajah Muthiah Medical College and Hospital, Annamalai Nagar. The animals were maintained according to the guidelines of the institutional animal ethical committee (IAEC). The study protocol and experiments were approved by IAEC.

After acclimatization for a period of 1 week, the animals were randomly divided into four groups consisting of six mice each. The following groups were maintained for a period of 60 days.

1. Control (CON) group: Mice of this group received control diet and olive oil, the vehicle (0.3 ml/kg/day, p.o) from the 16th day till the end of the experimental period.
2. HFFD group: Mice belonging to this group received HFFD and olive oil, the vehicle (0.3 ml/kg/day, p.o) from the 16th day till the end of the experimental period.
3. HFFD+ASX group: Mice belonging to this group received HFFD and were administered ASX in 0.3 ml olive oil (2 mg/kg b.w/day, p.o) from day 16 till the end of experimental period.
4. CON+ASX group: This group received control diet and were administered ASX (2 mg/kg b.w/day, p.o) in 0.3 ml olive oil from day 16 till the end of the experimental period.

Food and water were available ad libitum to the animals. HFFD had the following composition (g/100 g diet): 45.0 fructose, 10.0 ground nut oil, 10.0 beef tallow, 22.5 casein, 0.3 DL-methionine, 1.2 vitamin mixture, 5.5 mineral mixture, and 5.5 wheat bran. HFFD contained 45 % (w/w) fructose (39 % of calories), 20 % (w/w) fat (10 % beef tallow; 10 % groundnut oil; 40 % of calories), and 22.5 % (w/w) casein (21 % of calories). The standard laboratory chow consisted of 60 % (w/w) starch, 22.08 % (w/w) protein, and 4.38 % (w/w) fat. The normal chow diet provided 382.61 cal/100 g, while HFFD provided 471.25 cal/100 g. HFFD was prepared daily.

At the end of the experimental period, animals were fasted overnight, anesthetized the next day with ketamine hydrochloride (30 mg/kg, i.m.), and then killed by decapitation. Liver tissue was removed immediately and rinsed of any adhering blood with ice cold saline. Then, liver was quickly sliced, and tissue was homogenized in appropriate buffers and used for assays.

Determination of intracellular ROS production

Liver homogenate was suspended in HEPES buffered saline (pH 7.4 containing 140 mM NaCl, 5 mM KCl, 10 mM HEPES, 1 mM $CaCl_2$, 1 mM $MgCl_2$, and 10 mM glucose) and then treated with 10 μM DCFH-DA to make a final volume of 3 ml and incubated for 45 min. Conversion of nonfluorescent DCFH-DA to the highly fluorescent compound 2', 7'-dichlorofluorescein by ROS results in a change in fluorescence, which was measured using a spectrofluorometer with an excitation set at 485 nm and emission at 530 nm (Balasubramanyam et al. 2003).

Detection of lipid accumulation by Oil red O stain

Liver samples were frozen immediately after dissection, and the fresh frozen liver samples were cut in a cryostat, affixed to microscope slides, and air-dried at room temperature for 30 min. The liver sections were stained in fresh Oil red O for 10 min and rinsed in water. The slides were then viewed under the light microscope.

Western blot

Tissue processing

Liver tissue was homogenized in ice cold homogenization buffer (20 mM Tris–HCl, pH 7.4, 0.25 % SDS, 150 mM NaCl, 1 % NP-40, 0.5 % Triton X-100, 1 mM PMSF, 1 mM EDTA, and protease inhibitor cocktail) and centrifuged at $12,000 \times g$, for 15 min at 4 °C. The supernatant was used as the whole cell extract. For NF-κB expression study, the homogenate was processed to obtain cytosolic and nuclear fractions by the procedure outlined elsewhere (Sivakumar and Anuradha 2011). Protein concentrations of the extracts were measured (Lowry et al. 1951).

Liver homogenates containing equal amount of protein were resolved by 8–12 % SDS PAGE. The separated proteins were electrotransferred onto polyvinylidene fluoride membrane. The membranes were then blocked in Tris buffered saline-Tween 20 (TBST) solution (pH 7.4) containing 3 % bovine serum albumin for 2 h at room temperature and then incubated overnight at 4 °C with either anti-PERK, antiphospho-eIF2α, anti-phospho-JNK1(Cell signaling, USA), anti-XBP1 (Sigma-Aldrich, USA), anti-Bip (Santa Cruz, USA), anti-ATF6 (Santa Cruz, USA), anti-caspase 12 antibody (Sigma-Aldrich, USA), anti-IKK-β (Cell signaling, USA), antiphospho IKK-β (Cell signaling, USA) or anti-NF-κB (Santa Cruz, USA). After incubation with primary antibodies, the blots were washed with TBST and incubated with the respective secondary antibodies for 2 h at room temperature. Proteins were detected using chemiluminescent kit method (Enhanced ECL detection system, Thermoscientific, USA). The band intensities were quantified using Image J software. For normalization, the membranes were stripped of bound antibodies and reprobed with IKKB antibody for phospho IKKB, JNK1 antibody for phospho JNK1, and β-actin antibody for other proteins.

Statistical analysis

The values are statistically evaluated by one-way analysis of variance (ANOVA) followed by Tukey's multiple range test for multiple comparisons. A value of $p < 0.05$ was considered statistically significant. For ROS assay, the values are means (SD) of six mice, and for western blots, values are means (SD) from four mice.

Results

Effect of ASX on ROS production

Figure 1 represents the effect of ASX on the intracellular formation of ROS. In HFFD group, the fluorescence intensity of samples were significantly higher compared to control
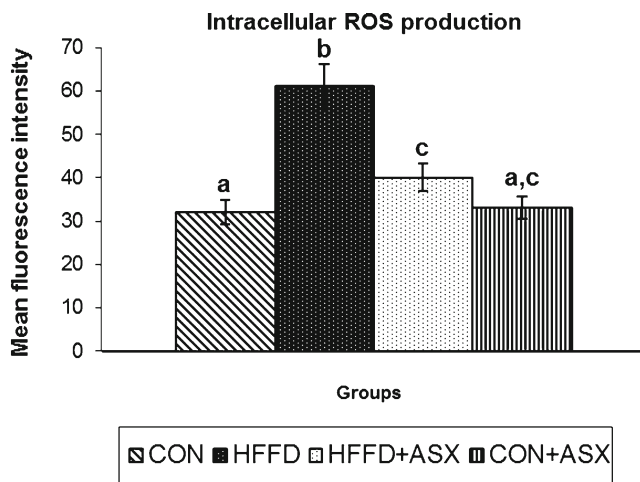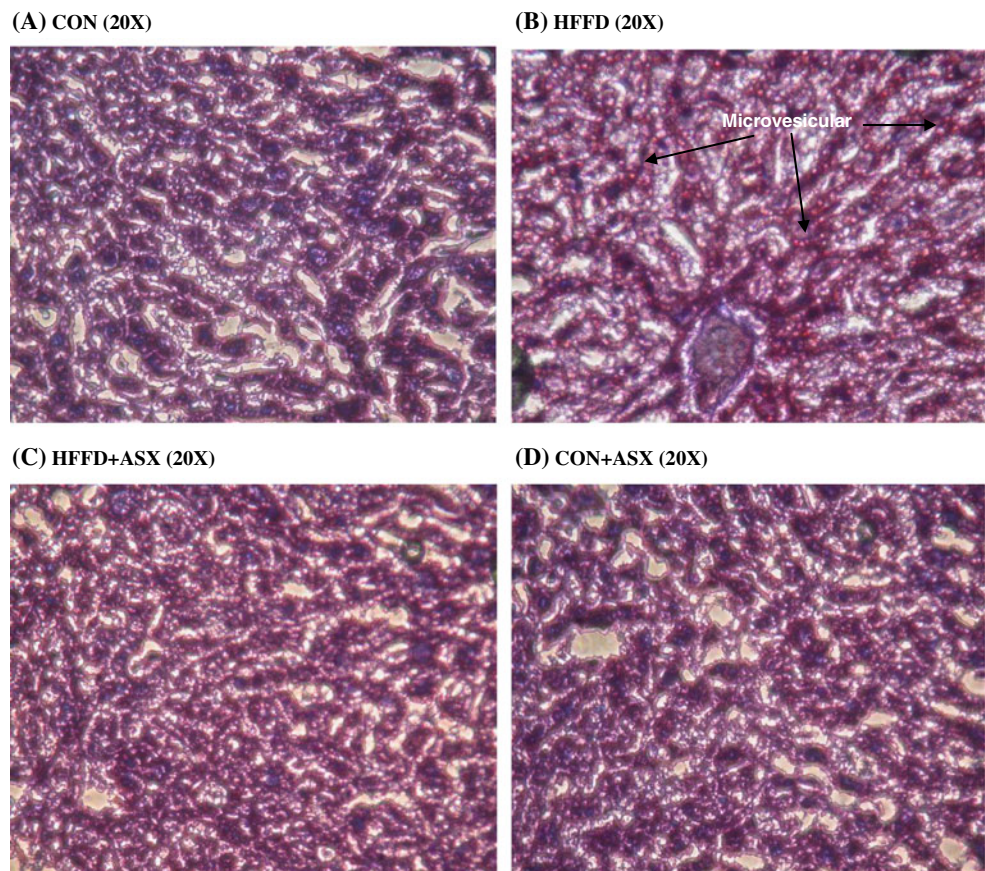
Intracellular ROS production

Fig. 1 Effect of ASX on intracellular production of ROS in liver tissue of experimental animals. Data are expressed as means (*SD*) for six mice. Values not carrying common superscript significantly differ from each other (ANOVA followed by Tukey's multiple range test ($p<0.05$))

group, indicating increased ROS production. ASX addition to HFFD-fed mice significantly reduced ROS production compared to untreated HFFD-fed mice ($p<0.05$). There was no significant difference between the fluorescent intensities of samples obtained from CON and CON+ASX groups.

Analysis of Oil red O staining of liver

Figure 2 shows the photomicrographs of Oil red O stained liver specimens. The histology of liver remains normal in the control group (Fig. 2a) and ASX-treated control group (Fig. 2d). In the HFFD group, the liver shows widespread deposition of lipid droplets inside the parenchymal cells (Fig. 2b). Liver from the HFFD+ASX group (Fig. 2c) showed limited and scattered droplets of fat when compared to HFFD group.

Effect of ASX on ER stress markers

To test whether ASX reduces ER stress, the expression of proteins such as PERK, p-eIF2α, XBP-1, ATF-6, and Bip were examined in hepatic tissues of animals by Western blotting.

Increased expression of PERK, p-eIF2α, ATF-6, and spliced XBP-1 protein (a marker for IRE-1 α activation) were observed in HFFD-fed mice compared to control group (Fig. 3). However, in ASX-treated HFFD fed mice, the expression was significantly reduced compared to HFFD. The expression of Bip was higher in HFFD group relative to control group. The increase in Bip was markedly reduced in ASX-treated HFFD group.

The expression of caspase-12, a specific mediator of ER stress-induced apoptosis was significantly upregulated in the

Fig. 2 Representative images of frozen liver sections stained with Oil red O (×20) of experimental animals. Section from CON group shows negligible red staining (**a**). HFFD fed mice liver (**b**) shows increased deposition of lipids. Red stained areas (arrows) indicate lipid deposition. Liver section of HFFD+ASX (**c**) shows reduced red staining indicating reduced lipid deposition as compared to HFFD. CON+ASX group (**d**) shows negligible staining similar to that of CON group (**a**)

HFFD group. However, the expression of caspase-12 was significantly lower after ASX treatment. There were no significant differences between CON and CON+ASX groups in the expression of ER stress markers (Fig. 3).

Effect of ASX on hepatic JNK1 phosphorylation

While HFFD feeding stimulated the expression of both total and p-JNK in mice liver, ASX addition significantly inhibited the upregulation of p-JNK and total JNK in HFFD-fed mice (Fig 4). There were no significant differences in the expression of p-JNK1 or JNK1 between ASX+CON and the CON groups.

Effect of ASX on hepatic IKKβ/NF-κB activation

The immunoblots of p-IKKβ and total IKKβ in mice liver are presented in Fig. 5a. Compared to the control group,

expression of p-IKKβ and IKKβ were significantly increased upon HFFD feeding. This increase was significantly reduced upon ASX supplementation to HFFD-fed mice.

Figure 6a and b represents the nuclear and cytoplasmic protein abundance of NF-κB p65 in liver. The data reveals that NF-κB p65 expression was significantly lower in the cytosolic fraction (Fig. 6b) but higher in the nuclear fraction (Fig 6a) obtained from the liver of HFFD-fed mice compared to the respective fractions from control group. This observation confirms the translocation of NF-κB into the nucleus from cytoplasm in the liver of HFFD-fed mice. Supplementation of ASX to HFFD-fed mice caused a significant reversal, i.e., reduction in the expression of NF-κB in nuclear fraction and a simultaneous increase in cytosolic fraction compared to HFFD-fed mice, indicating that NF-κB activation and translocation are prevented in presence of ASX.

Fig. 3 Representative protein expression of Bip, XBP-1, PERK, P-eIF2α, ATF-6, Caspase-12, and β-actin. Data are expressed as fold change with respect to control and are mean (*SD*) for four mice. Values not carrying common superscript significantly differ from each other. (ANOVA followed by Tukey's multiple range test ($p<0.05$))
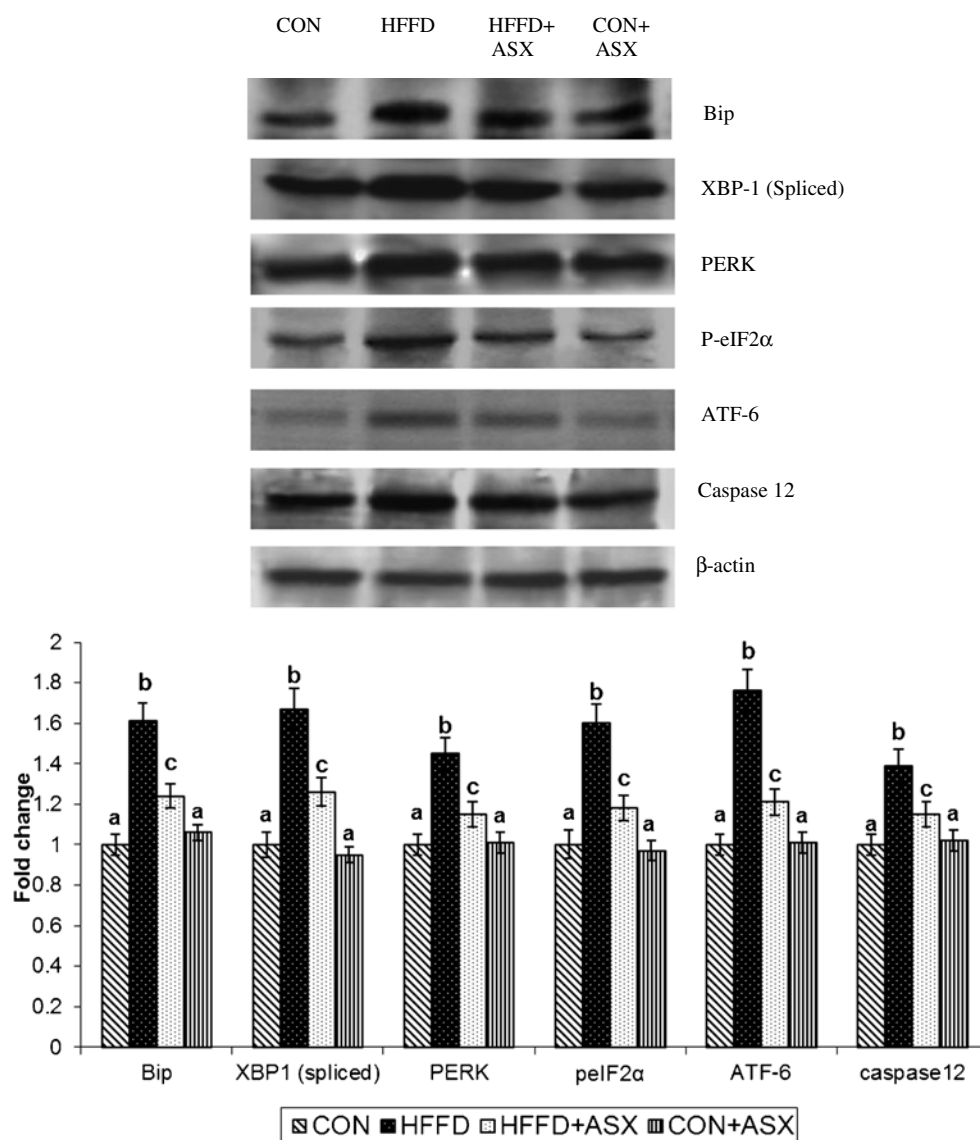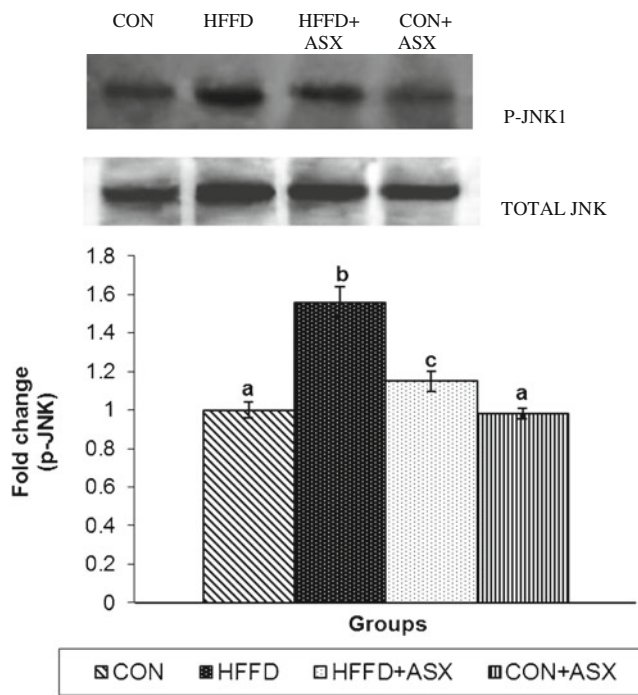
Fig. 4 Effect of ASX on JNK phosphorylation in the liver of experimental animals. For determining the extent of JNK activation, proteins were immunoblotted with anti-p-JNK antibody. Blots were stripped and reprobed with an anti-JNK antibody. After normalization of phospho form with total protein, the values (mean (SD) for four mice) are expressed as fold change with respect to control. (ANOVA followed by Tukey's multiple range test ($p<0.05$))

Fig. 5 Effect of ASX on IKK-β phosphorylation in liver of experimental animals (a). For determining the extent of IKK-β activation, proteins were immunoblotted with anti-p-IKK-β antibody. Blots were stripped and reprobed with an anti-IKK-β antibody. After normalization of phosphoform with total protein, the values (mean (SD) for four mice) are expressed as fold change with respect to control. (ANOVA followed by Tukey's multiple range test ($p<0.05$))

Discussion

The current study reports the induction of hepatic inflammation and ER stress in a diet-induced obese mouse model of insulin resistance and the reversal of these processes by ASX.

Increased level of the ER chaperone Bip in HFFD group suggests ER stress. This increase was associated with amplified levels of PERK, ATF6, and XBP-1. The phosphorylation status of eIF2α, a downstream target of PERK, was also increased. Caspase-12, the hallmark of ER-associated apoptosis, was also overexpressed.

Pathological nutrient excess as in obesity has been shown to interfere with normal ER function causing deviant protein folding, which results in adaptive ER stress. Expression level of Bip, an immunoglobulin binding protein was much higher in the liver of obese diabetic mice compared to nondiabetic C57BL6 mice (Nakatani et al. 2005). Studies in both high fat-fed and ob/ob (leptin-deficient) mice models of obesity have noticed increased expression of PERK and eIF2α and Bip in liver (Boden et al. 2008). Nutritional manipulations such as fasting and refeeding result in altered phosphorylation status of eIF2α (Oyadomari et al. 2008). Interestingly, ASX markedly prevented the upregulation of the ER stress markers induced by HFFD.
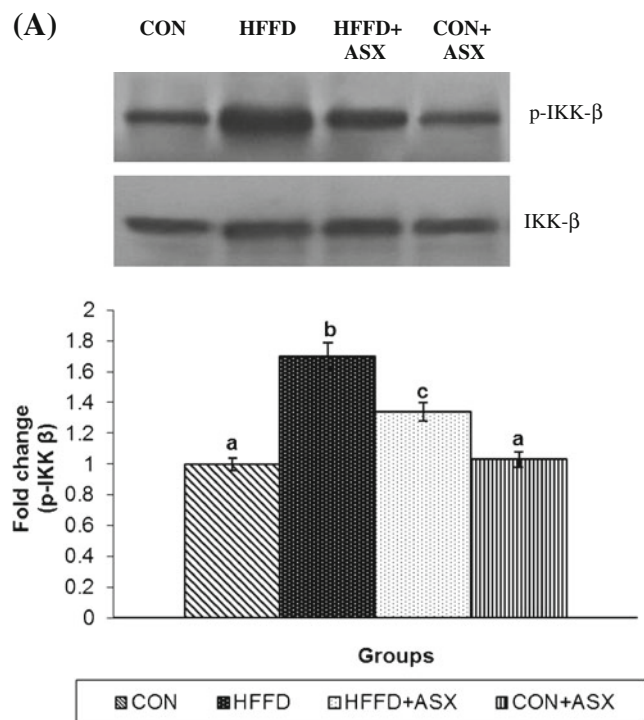
Studies in animal models of insulin resistance and fatty liver have demonstrated that hepatic steatosis and ER stress are linked to each other (Boden et al. 2008). Activated eIF2α and PERK enhance lipogenesis by inducing C/EBPα and β and by activating sterol regulatory element binding protein. Independent of PERK, XBP1, the transcription factor downstream of IRE1 activation, promotes de novo lipid synthesis through C/EBPα and β in the liver in high carbohydrate diet-fed rats. Transgenic mice with eIF2α-phosphorylation defect exhibit reduced hepatosteatosis and greater insulin sensitivity compared to wild-type mice when fed a high fat diet (Oyadomari et al. 2008).

While ER stress can result in lipogenesis, lipids and defects in metabolism can induce ER stress (Fu et al. 2011; Gentile et al. 2011; Guo et al. 2007; Wei et al. 2006). Saturated fatty acids (SFAs) such as palmitate and stearate modulate survival and apoptotic signals through ER stress in various cell types (Guo et al. 2007; Wei et al. 2006). One study found that increase in SFA content and PC/PE ratio in ER lipids in obese rat led to Ca^{2+} retention, causing protein misfolding and ER stress (Oyadomari et al. 2008). Proteomic and lipidomic analysis of ER from liver revealed the abundance of enzymes of lipid metabolism and downregulation of protein synthesizing machinery in obese rats as compared to those from lean rats.

Fig. 6 Effect of ASX on NFκB expression in nuclear (**a**) and cytoplasmic (**b**) fractions in liver of experimental animals was assessed by immunoblotting with anti-NFκB antibody. Blots were stripped and reprobed with an anti-β-actin antibody (loading control). The bands were quantified and then normalized with β-actin. Values are expressed as fold change with respect to control. Data are expressed as mean (*SD*) for four mice. Values not carrying common superscript significantly differ from each other. (ANOVA followed by Tukey's multiple range test ($p < 0.05$)])
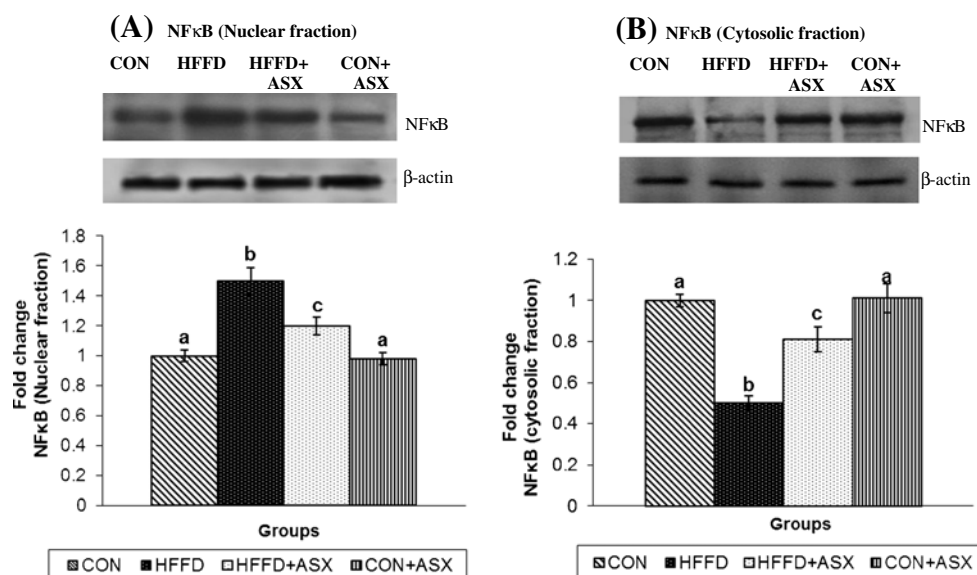
This suggests that ER starts to perform lipid synthesis and lipid metabolism functions in obesity rather than being a site of protein synthesis (Fu et al. 2011). Thus, hepatic ER stress can promote de novo lipogenesis, while lipids can exacerbate ER stress, a situation that creates a vicious cycle.

Accumulation of lipids in the liver in HFFD could, thus, be a cause and an outcome of ER stress in this model. Limited deposition of lipid droplets inside the parenchymal cells observed in HFFD+ASX group compared to HFFD group substantiates our earlier finding that ASX reduces liver lipid levels in obese mice (Arunkumar et al. 2012). Decreased lipid accumulation may account for the inhibition of ER stress in the liver and vice versa.

NF-κB, a heterodimer of p50 and p65 subunits, remains inactive in the cytosol in complex with inhibitor of NF-κB (IκB) under normal condition. Upon stimulation by proinflammatory cytokines, ROS or mitogens, IκB undergoes phosphorylation by IκB kinase β (IKKβ) and degradation via the ubiquitin proteasome pathway. Dissociation of IκB from the p50/p65 heterodimer exposes the nuclear localization signals on NF-κB, which subsequently translocates to the nucleus and regulates the transcription of numerous inflammatory genes. IKKβ in its active form is known to induce serine phosphorylation of IRS1 at Ser 307 and block insulin signaling. These observations correlate with our previous study, which showed decreased tyrosine phosphorylation and increased serine phosphorylation of both IRS1 and 2 in HFFD-fed group (Bhuvaneswari and Anuradha 2012). HFFD feeding resulted in the upregulation of p-IKKβ and nuclear translocation of NF-κB. This could be attributed to the prevailing ER stress, since the IRE-1-TRAF2-ASK1 complex can activate NF-κB. ASX treatment effectively suppressed IKKβ phosphorylation and nuclear translocation of NF-κB p65 subunit. Lee et al. (Lee et al. 2008) found that ASX inhibits inflammatory gene expression by suppressing IKKβ-dependent NF-κB

activation. Thus, suppression of IKK-β and p-IKK-β by ASX provides evidence for its antiinflammatory action.

ER stress is also a major source for the production of ROS. Accumulation of unfolded proteins in the ER produces ROS through several mechanisms. Activated Bip stimulates mitochondrial oxidative phosphorylation to produce ROS as a by-product. ROS production can also occur during disulphide bond formation that involves transfer of electrons from thiol groups of substrates through protein disulfide isomerase, an enzyme which catalyzes disulphide bridge formation (Benjamin and Weissman Jonathan 2004). Reduction in glutathione due to consumption during disulphide bond formation may also contribute to ROS production (Cuozzo and Kaiser 1999).

The link between ER stress, insulin action, and type 2 diabetes has been postulated by Ozcan et al. (Ozcan et al. 2004). They suggest that ER is the proximal site that senses nutritional excess and translates it into metabolic and inflammatory responses. Lee et al. observed elevation in ER stress markers in liver and adipose tissue and loss of XBP-1 in mouse models of obesity and in cell culture (Lee et al. 2008). This was accompanied by increase in JNK activity and serine phosphorylation of IRS-1. They also proved that IRE-1α is involved in the inhibition of insulin action through JNK. Furthermore, pretreatment of Fao cells with tunicamycin, an inhibitor of ER stress or suppression of JNK activity with a synthetic inhibitor, SP600125, reversed ER stress-induced serine phosphorylation of IRS-1 (Kaneto et al. 2006). Taken together, these findings suggest that JNK1 is a downstream effector of ER stress, activation of which results in the inhibition of insulin action and deterioration of glucose homeostasis resulting in T2D.

The JNK pathway is known to be activated by several factors such as oxidative stress, free fatty acids, and tumor necrosis factor-α, all of which are shown to be increased during

HFFD-induced insulin resistance (Bhuvaneswari et al. 2010). Suppression of JNK pathway by ASX could counterbalance the deleterious outcome of ER stress.

In aggregate, we have shown that ASX targets the liver and breaks the vicious cycle between lipid overload, ROS production, ER stress, and JNK activation in high fat and high fructose-induced model of IR. These findings provide a mechanistic insight into the insulin sensitivity effects of ASX reported earlier by us in this model (Bhuvaneswari et al. 2010; Arunkumar et al. 2012; Bhuvaneswari and Anuradha 2012).

Our findings may have important implications in context of a recent study by Lee et al., who reported that the compound ASX induces the expression of heat shock proteins (Hsps)70 and heme oxygenase (HO)-1 in SH-SY5Y human neuroblastoma cells (Lee et al. 2010). Impaired insulin signaling reduces the expression of Hsps, and the chaperone HO is low in tissues of diabetic animals allowing the accumulation of harmful protein aggregates (Hooper and Hooper 2009). Hsp70 and HO block the activation of inflammatory kinases like JNK (Chung et al. 2008) and the transcription factor NF-kB (Stice and Knowlton 2008). Restoring insulin action raises Hsps in diabetic animal models, while increasing Hsps would decrease inflammation and insulin action. Thus, the beneficial effects of ASX might also involve Hsp induction, which needs further investigation in HFFD-induced diet model.

References

Arunkumar E, Bhuvaneswari S, Anuradha CV (2012) An intervention study in obese mice with astaxanthin, a marine carotenoid—effects on insulin signaling and proinflammatory cytokines. Food Funct 3:120–126

Balasubramanyam M, Koteswari AA, Sampath Kumar R et al (2003) Curcumin induced inhibition of reactive oxygen species generation: novel therapeutic implications. J Biosci 28:715–721

Benjamin PT, Weissman Jonathan S (2004) Oxidative protein folding in eukaryotes: mechanisms and consequences. J Cell Biol 164:341–346

Bhuvaneswari S, Anuradha CV (2012) Astaxanthin prevents loss of insulin signaling and improves glucose metabolism in liver of insulin resistant mice. Can J Physiol Pharmacol 90:1544–1552

Bhuvaneswari S, Arunkumar E, Viswanathan P, Anuradha CV (2010) Astaxanthin restricts weight gain, promotes insulin sensitivity, and curtails fatty liver disease in mice fed with obesity promoting diet. Process Biochem 45:1406–1414

Boden G, Duan X, Homko C, Molina EJ, Song W, Perez O, Cheung P, Merali S (2008) Increase in endoplasmic reticulum stress-related proteins and genes in adipose tissue of obese and insulin-resistant individuals. Diabetes 57:2438–2444

Chung J, Nguyen AK, Henstridge DC, Holmes AG, Chan MH, Mesa JL, Lancaster GI, Southgate RJ, Bruce CR, Duffy SJ, Horvath I, Mestril R, Watt MJ, Hooper PL, Kingwell BA, Vigh L, Hevener A,

Febbraio MA (2008) HSP72 protects against obesity-induced insulin resistance. Proc Nat Acad Sci 105:1739–1744

Cuozzo JW, Kaiser A (1999) Competition between glutathione and protein thiols for disulphide bond formation. Nat Cell Biol 1:130–135

Deng J, Lu PD, Zhang Y, Scheuner D, Kaufman RJ, Sonenberg N, Harding HP, Ron D (2004) Translational repression mediates activation of nuclear factor kappa b by phosphorylated translation initiation factor 2. Mol Cell Biol 24(23):10161. doi:10.1128/MCB.24.23.10161-10168.2004

Draznin B (2006) Molecular mechanisms of insulin resistance: serine phosphorylation of insulin receptor substrate-1 and increased expression of p85alpha: the two sides of a coin. Diabetes 55:2392–2397

Fu S, Yang S, Li P, Hofmann O, Dicker L, Hide W, Lin X, Watkins SM, Ivanov AR, Hotamisligil GS (2011) Aberrant lipid metabolism disrupts calcium homeostasis causing liver endoplasmic reticulum stress in obesity. Nature 473:528–531

Gentile CL, Frye MA, Pagliassotti MJ (2011) Fatty acids and the endoplasmic reticulum in nonalcoholic fatty liver disease. Biofactors 37:8–16

Gregor MF, Hotamisligil GS (2007) Adipocyte stress: the endoplasmic reticulum and metabolic disease. J Lipid Res 48:1905–1914

Guerin M, Huntley ME, Olaizola M (2003) Haematococcus astaxanthin: applications for human health and nutrition. Trends Biotechnol 21:210–216

Guo W, Wong S, Xie S, Lei T, Luo Z (2007) Palmitate modulates intracellular signaling, induces endoplasmic reticulum stress, and causes apoptosis in mouse 3T3-L1 and rat primary preadipocytes. Am J Physiol Endrocrinol metab 293:E576–E586

Hooper PL, Hooper PL (2009) Inflammation, heat shock proteins, and type 2 diabetes. Cell Stress Chaperones 14:113–115

Hooper PL, Hooper PL, Tytell M, Vígh L (2010) Xenohormesis: health benefits from an eon of plant stress response evolution. Cell Stress Chaperones 15:761–770

Hotamisligil GS (2010) Endoplasmic reticulum stress and the inflammatory basis of metabolic disease. Cell 140:900–917

Ikeuchi M, Koyama T, Takahashi J, Yazawa J (2007) Effects of astaxanthin in obese mice fed a high-fat diet. Biosci Biotechnol Biochem 71:893–899

Kaneto H, Nakatani Y, Kawamori D, Miyatsuka T, Matsuoka T, Matsuhisa M, Yamasaki Y (2006) Role of oxidative stress, endoplasmic reticulum stress, and c-Jun N-terminal kinase in pancreatic β-cell dysfunction and insulin resistance. Int J Biochem Cell Biol 38:782–793

Lebovitz HE (2001) Insulin resistance: definition and consequences. Exp Clin Endocrinol Diabetes 109:135–148

Lee AH, Scapa EF, Cohen DE, Glimcher LH (2008) Regulation of hepatic lipogenesis by the transcription factor XBP1. Science 320:1492–1496

Lee DH, Lee YJ, Kwon KH (2010) Neuroprotective effects of astaxanthin in oxygen–glucose deprivation in SH-SY5Y cells and global cerebral ischemia in rat. J Clin Biochem Nutr 47:121–129

Lowry OH, Rosebrough NJ, Farr AL, Randall RJ (1951) Protein measurement with the folin phenol reagent. J Biol Chem 193:265–275

Malhotra JD, Miao H, Zhang K, Wolfson A, Pennathur S, Pipe SW, Kaufman RJ (2008) Antioxidants reduce endoplasmic reticulum stress and improve protein secretion. Proc Natl Acad Sci USA 105:18525–18530

Nakatani Y, Kaneto H, Kawamori D, Yoshiuchi K, Hatazaki M, Matsuoka TA, Ozawa K, Ogawa S, Hori M, Yamasaki Y, Matsuhisa M (2005) Involvement of endoplasmic reticulum stress in insulin resistance and diabetes. J Biol Chem 280:847–851

Oyadomari S, Harding HP, Zhang Y, Oyadomari M, Ron D (2008) Dephosphorylation of translation initiation factor 2 alpha enhances

glucose tolerance and attenuates hepatosteatosis in mice. Cell Metab 7:520–532

Ozcan U, Cao Q, Yilmaz E, Lee H, Iwakoshi NN, Ozdelen E, Tuncman G, Görgün C, Glimcher LH, Hotamisligil GS (2004) Endoplasmic reticulum stress links obesity, insulin action, and type 2 diabetes. Science 306:457–461

Perseghin G, Petersen K, Shulman GI (2003) Cellular mechanism of insulin resistance: potential links with inflammation. Int J Obes Relat Metab Disord 27(3):S6–S11

Schaffer JE (2003) Lipotoxicity: when tissues overeat. Curr Opin Lipidol 14:281–287

Shoelson SE, Lee J, Yuan M (2003) Inflammation and the IKK beta/I kappa B/NF-kappa B axis in obesity- and diet-induced insulin resistance. Int J Obes Relat Metab Disord 27(3):S49–S52

Sivakumar AS, Anuradha CV (2011) Effect of galangin supplementation on oxidative damage and inflammatory changes in fructose-fed rat liver. Chem Biol Interact 193:141–148

Stice JP, Knowlton AA (2008) Estrogen, NF-kappaB, and the heat shock response. Mol Med 14:517–527

Tanti JF, Jager J (2009) Cellular mechanisms of insulin resistance: role of stress-regulated serine kinases and insulin receptor substrates (IRS) serine phosphorylation. Curr Opin Pharmacol 9:753–762

Uchiyama K, Naito Y, Hasegawa G, Nakamura N, Takahashi J, Yoshikawa T (2002) Astaxanthin protects beta-cells against glucose toxicity in diabetic db/db mice. Redox Rep 7:290–293

Vidhyavathi R, Venkatachalam L, Sarada R, Ravishankar GA (2008) Regulation of carotenoid biosynthetic genes expression and carotenoid accumulation in the green alga *Haematococcus pluvialis* under nutrient stress conditions. J Exp Bot 59:1409–1418

Wei Y, Wang D, Topczewski F, Pagliassotti MJ (2006) Saturated fatty acids induce endoplasmic reticulum stress and apoptosis independently of ceramide in liver cells. Am J Physiol Endrocrinol Metab 291:275–281

Yalcin W, Hotamisligil GS (2013) Impact of ER protein homeostasis on metabolism. Diabetes 62:691–693